



Modelling of Damage During Hot Forging of Ingots

Christiansen, Peter; Hattel, Jesper Henri; Bay, Niels; Martins, Paolo A.F.

Published in:
STEELSIM 2013 - The 5th International Conference

Publication date:
2013

[Link back to DTU Orbit](#)

Citation (APA):
Christiansen, P., Hattel, J. H., Bay, N., & Martins, P. A. F. (2013). Modelling of Damage During Hot Forging of Ingots. In *STEELSIM 2013 - The 5th International Conference*

General rights

Copyright and moral rights for the publications made accessible in the public portal are retained by the authors and/or other copyright owners and it is a condition of accessing publications that users recognise and abide by the legal requirements associated with these rights.

- Users may download and print one copy of any publication from the public portal for the purpose of private study or research.
- You may not further distribute the material or use it for any profit-making activity or commercial gain
- You may freely distribute the URL identifying the publication in the public portal

If you believe that this document breaches copyright please contact us providing details, and we will remove access to the work immediately and investigate your claim.

Modelling of Damage During Hot Forging of Ingots

Peter Christiansen, Jesper H. Hattel, Niels Bay, Department of Mechanical Engineering, Technical University of Denmark, DTU – Building 425, DK-2800 Kgs. Lyngby, Denmark, **Paulo A. F. Martins**, Instituto Superior Tecnico, University of Lisbon, Av. Rovisco Pais, 1049-001 Lisboa, Portugal
petc@mek.dtu.dk

Ductile damage modelling in the ingot forging process is discussed. Advantages and disadvantages of both coupled and uncoupled ductile damage models are presented. Some uncoupled damage models are examined in greater detail regarding their applicability to different processes, where hydrostatic compression as well as tension, combined with shear stresses, are present. It is shown that the numerical implementation can influence the results substantially and therefore lead to software user dependent conclusions. It may be advantageous for the user of commercial finite element programs to base the damage analysis on the Cockcroft & Latham criterion, since this with changing cut-off value does not inconsistently change the location of damage, in contradiction to the other investigated criteria, and since it is able to predict damage in processes, which are slightly compressive.

1. Introduction to ingot forging

The ingot forging process (also known as cogging when performing multiple forging operations on the same component) is utilized for manufacturing large steel parts such as shafts, which are used in wind turbines, ship's propulsion or power plants. Failure of such components during their service life is expensive and should be avoided. The mechanical soundness of the manufactured shafts is therefore important. The mechanical properties, especially regarding fatigue lifetime and fracture toughness, are affected by the manufacturing process. It is of interest to address the manufacturing procedure in order to understand its influence on final shaft properties.

Large shafts are manufactured by first casting a large metallic block, known as an ingot. The weight of the cast ingot can be several hundred tons depending on the size of the final part. The ingot casting process may give rise to a number of defects such as coarse microstructure due to long cooling time, segregations if casting alloyed steel, slag inclusions or porosities due to improper feeding or gas entrapment. According to ASM Handbook [1] some of these defects can be minimized by substantial hot forging of the cast ingot. Coarse microstructure can be refined by deformation enhanced recrystallization, slags can be crushed to smaller particles and porosities can be closed by deformation. The practical experience of Nasmyth [1] allowed him to make conclusions about the importance of the shape of the forging dies. He found that a V-shaped lower die was superior to a flat lower die as regards closure of internal defects and ensuring mechanical soundness of the forged ingots.

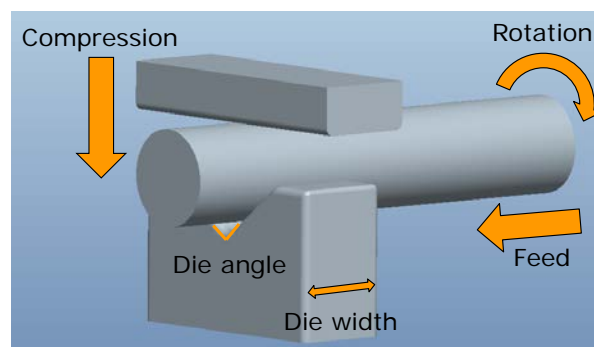


Fig. 1 Principal sketch of the ingot forging process with process variables

A principal sketch of the ingot forging process can be seen in Fig. 1. It consists of local, stepwise compressions of a cross-section of the ingot between an upper plane die and a V-shaped lower die. The ingot is rotated in between each compression step. After finishing a local cross-section of the ingot, it is displaced forward between the open dies and a new cross-section is forged. The ingot is preheated to a temperature of approximately 1200°C before forging.

A major objective of the hot forging procedure is to cure internal defects created during the casting process, and it is important to ensure that ductile damage is not induced during the procedure. This may be examined by damage modelling in numerical simulation of the forging process. Induced damage may be estimated by either coupled or

uncoupled ductile damage modelling. In this paper, the main emphasis is placed on uncoupled damage models, which are adopted for ingot forging with lower V-shaped dies of different die angles.

2. Ductile damage modelling

2.1 Coupled ductile damage models

In a coupled damage model the value quantifying damage influences the mechanical properties of the material being formed, which implies a coupling between accumulated damage and the mechanical properties of the material.

Kuhn and Downey [2], Green [3] and Gurson-Tvergaard-Needleman [4] propose porous plasticity based models, where the yield surface of the material is modified depending on the density of the material. The models include an evolution algorithm for the material density depending on deformation history. Accumulated damage is thereby modelled as a loss in density, which reflects the preliminary stage of failure before fracture, localizing the formation of internal cracks and porosities.

Modelling of ductile damage was originally introduced by Kachanov [5]. The basic idea being that an internal variable is used as measure of the damage. The internal variable is used to describe the gradual degrading of the material due to formation of internal porosities and thereby diminishing the mechanical properties. The variable can for instance, as in the model of Lemaitre [6], be a function of stress-strain history or, as in the model by Xue & Wierzbicki [7], also be dependent on the Lode-parameter.

If fully coupled models are used in an FEM simulation, it may increase computational time considerably. The maximum allowable timestep may be reduced for explicit codes or the solution may “drift” due to the explicit time integration. On the other hand if an implicit code is utilized, the number of iterations needed for convergence may increase significantly. Usually these coupled finite element models also contain a number of constants, which may be difficult to determine experimentally. On the other hand a fully coupled simulation ensures the influence of damage on strength.

2.2 Uncoupled ductile damage modelling

Uncoupled ductile damage modelling usually consists of integrating some stress measure through strain history:

$$C = \int f(\sigma_{ij}) g(d\varepsilon_{ij}^{pl}) \quad (1)$$

where C is the accumulated damage value, $f(\sigma_{ij})$ is a function of the stress tensor and $g(d\varepsilon_{ij}^{pl})$ is a function of the plastic strain tensor. Uncoupled means that the value of C does not have an influence on the mechanical properties of the material, hence damaged materials do not have a lower strength than an undamaged material. This makes these criteria easy to implement since they are basically applied in a post-processing operation of the numerical analysis, which do not require for instance added equilibrium iterations. Semi-coupled approaches do also exist, where the material properties are gradually reduced as C increases. This reduction is however only performed after the equilibrium iterations have been performed during each deformation step. These semi-coupled approaches are not considered further in the present work.

A number of uncoupled damage models have been proposed to simulate ductile damage in metal forming. An early ductile damage model was proposed by Freudenthal [8]:

$$C = \int \bar{\sigma} d\bar{\varepsilon}^{pl} \quad (2)$$

Freudenthal's criterion (2) is a simple integration of the effective stress $\bar{\sigma}$ with respect to the effective plastic strain $\bar{\varepsilon}^{pl}$, hence it can be interpreted as a plastic work criterion.

An advancement from Freudenthal's criterion is the criterion suggested by Cockcroft & Latham [9]:

$$C = \int \sigma_I d\varepsilon^{pl} \quad (3)$$

Instead of integrating the effective stress $\bar{\sigma}$, as in Freudenthal's criterion, the largest principal stress σ_I is integrated. Often a normalized version of the Cockcroft & Latham criterion is used:

$$C = \int \frac{\sigma_I}{\bar{\sigma}} d\varepsilon^{pl} \quad (4)$$

In contrast to the three previous fracture criteria, which are empirically based, Oyane [10] derived a criterion based on porous metal plasticity:

$$C = \int \left(1 + \frac{I}{a_0} \frac{\sigma_m}{\bar{\sigma}} \right) d\bar{\epsilon}^{pl} \quad (5)$$

The Oyane criterion (5) introduces a dependence on hydrostatic stress $\sigma_m = \sigma_{kk}/3$ and the constant a_0 . A damage criterion based on growth of spherical porosities is given by Rice & Tracey [11]:

$$C = \int \exp \left(\frac{3}{2} \frac{\sigma_m}{\bar{\sigma}} \right) d\bar{\epsilon}^{pl} \quad (6)$$

It should be noticed that several other uncoupled ductile damage criteria exists such as, e.g. Brozzo et al. [12] and Ayada et al. [13]. They are however not analysed in the present work.

2.3 Discussion of uncoupled ductile damage criteria

The Freudenthal criterion (2) predicts same degree of damage for a plastic material, which experiences same equivalent plastic strain regardless whether the loading is compressive or tensile. This is in disagreement with the experimental findings of Bridgman [14], who noted that materials formed under hydrostatic compression have a marked increase in formability as compared to materials formed under hydrostatic tension. Freudenthal's criterion is therefore disregarded for the rest of the paper.

To be in accordance with Bridgman's findings the Cockcroft & Latham criterion (3)-(4) is normally only accumulating damage, when the largest principal stress $\sigma_I > 0$. This implies that the criterion can accumulate damage even for moderate, negative hydrostatic stress states. In case of plane strain or plane stress conditions, the cut-off value for the accumulation of positive damage is $\sigma_m = -\bar{\sigma}/2$ and $\sigma_m = -\bar{\sigma}/3$ respectively. Adopting either Oyane's (5) or Rice & Tracey's (6) damage criterion, accumulation of damage is normally only done, when the hydrostatic stress is positive. Some commercial finite element computer programs like DEFORM [15] do allow for accumulation of negative damage similar to a porous plasticity model, i.e. assuming ductile damage to be reversible. This possibility is not considered in the present work because it suffers from consistency with the empirical foundations behind the development of some of the uncoupled damage functions. Hence damage accumulation can only increase or remain constant but not decrease.

Since both the Oyane and the Rice & Tracey criteria incorporates the ratio between hydrostatic stress and flow stress, it may be advantageous for the understanding to list some simple cases of stress states to obtain a better understanding of the damage criteria and the accumulation of damage depending on hydrostatic stress.

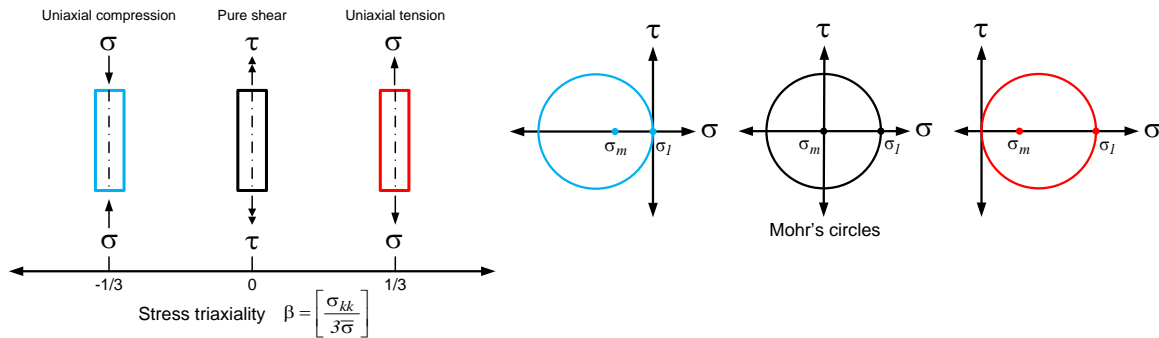


Fig. 2 Three plane stress metal forming operations and corresponding Mohr's circles.

Fig. 2 shows the three fundamental stress states: Uniaxial compression, pure shear and uniaxial tension of a round bar. The corresponding Mohr's circles are shown indicating largest principal stress σ_I and hydrostatic stress σ_m . The parameter β is the so-called stress triaxiality, originally introduced by Vujovic & Shabaik [16], and in this article defined as $\beta = \sigma_{kk}/3\bar{\sigma}$.

In the following the influence of cut-off value on the accumulation of damage is analysed adopting models based on largest principal stress and stress triaxiality. For simplicity $a_0 = 1$ is assumed in the Oyane criterion.

2.3.1 Cut-off value 1

Damage is accumulated with the Cockcroft & Latham criteria, if $\sigma_I > 0$ and with the Oyane and Rice & Tracey criteria, if $\beta > 0$. With the selected damage value Table 1 lists, for different ranges of β , whether or not the different damage criteria predict an increase in ductile damage, when plane stress is assumed.

Table 1 Damage accumulation as function of cut-off value 1

	Cockcroft & Latham	Oyane	Rice & Tracey
$\beta \leq -1/3$	No	No	No
$-1/3 < \beta \leq 0$	Yes	No	No
$\beta > 0$	Yes	Yes	Yes

It is seen that slightly negative values of stress triaxiality causes damage accumulation with the Cockcroft & Latham criterion, while the two other criteria do not. All criteria, however, have a lower limit in stress triaxiality, below which damage is not accumulated.

2.3.2 Cut-off value 2

For a cut-off value of 2 damage is accumulated with the Cockcroft&Latham criteria, if $\sigma_I > 0$ and with the Oyane and Rice & Tracey criteria, if $\beta \geq 0$.

Table 2 Damage accumulation as function of cut-off value 2

	Cockcroft & Latham	Oyane	Rice & Tracey
$\beta \leq -1/3$	No	No	No
$-1/3 < \beta < 0$	Yes	No	No
$\beta \geq 0$	Yes	Yes	Yes

The main difference between cut-off values 1 and 2, Table 1 and Table 2, is that the Oyane and the Rice & Tracey criteria both predict damage accumulation in pure shear deformation processes ($\beta = 0$), when cut-off value is 2 but not 1. However damage is not accumulated with the two criteria for even minor hydrostatic pressures.

2.4 Cut-off value 3

The Cockcroft & Latham, Oyane and Rice & Tracey criteria all require the integral in the damage formula to be positive.

Table 3 Damage accumulation as function of cut-off value 3

	Cockcroft & Latham	Oyane	Rice & Tracey
$\beta \leq -1$	No	No	Yes
$-1 < \beta \leq -1/3$	No	Yes	Yes
$-1/3 < \beta$	Yes	Yes	Yes

Table 3 shows that for a cut-off value equal to 3 the Rice & Tracey criterion predicts accumulation of damage for all stress triaxiality ranges. This is in disagreement with coupled porous plasticity models, that predict densification, which implies closure of internal porosities and an increase in mechanical strength, with increased compressive stress triaxiality. It is also problematic, if the finite element code has semi-coupled damage, where the mechanical strength is gradually reduced as damage is accumulated. However it should also be noticed, that since $\exp(x) \rightarrow 0$ for $x \rightarrow -\infty$, the accumulated damage becomes small for highly compressive hydrostatic stress states.

The Oyane criterion also predicts accumulation of damage for quite compressive stress triaxialities. This can be diminished by choosing a large value for a_0 , but that will also diminish the damage accumulation for positive stress triaxialities and therefore reduce the Oyane criterion to simply predict fracture at some effective plastic strain value regardless of the stress state. The criterion will thus have the same problem as the Freudenthal criterion, where the difference in damage in mainly compressive or tensile stress state is not reflected in the predicted damage value. On the contrary to the Oyane and the Rice & Tracey criteria, the Cockcroft & Latham criteria is in principle unaffected by choice of cut-off value.

3. Numerical simulation

In order to illustrate the performance of uncoupled ductile damage modelling in forging, both upsetting of a flanged specimen and an ingot forging process is simulated using the finite element flow formulation, which is based on the following weak form:

$$\int_V \bar{\sigma} \delta \dot{\epsilon}^{pl} dV + K \int_V \dot{\epsilon}_V^{pl} \delta \dot{\epsilon}_V^{pl} = \int_S \tau_i \delta u_i dS \quad (7)$$

where V is the control volume limited by surfaces S_u and S_f , where velocities u_i and surface tractions τ_i are prescribed, $\bar{\sigma}$ is the effective stress, $\dot{\epsilon}^{pl}$ is the effective plastic strain-rate, K is a large constant penalizing volumetric plastic strain-rate, $\dot{\epsilon}_V^{pl} = \dot{\epsilon}_{kk}^{pl}$ is the volumetric strain-rate. Friction is modelled using the constant friction model $\tau = m_f k$, where $0 \leq m_f \leq 1$ is the friction factor and k is the shear flow stress. Both full and reduced integration schemes are utilized in the numerical implementation. A thorough introduction to the finite element flow formulation may be found in Nielsen et al. [17].

Two different processes are numerically modelled: upsetting of a flanged specimen and ingot forging. The purpose of modelling flange upsetting is to illustrate differences in predicted ductile damage depending on the choice of cut-off value for the damage criteria. Numerical simulations are performed based on the experimental work of Gouveia et al. [18].

Modelling of the ingot forging process is of interest because the products are very large, which implies that experimental findings using traditional destructive sectioning of full size ingots in order to investigate defects evolution due to forging, is impracticable due to the large expenses. The numerical simulation is applied to investigate whether a forging operation is likely to cause unacceptable ductile damage. It is thus important to clarify, how a ductile damage criterion should be implemented/applied in the numerical simulation software. This is investigated by modelling the real physical experiment and analysing consequences of the numerical implementation.

3.1 Numerical simulation of the upsetting of a flanged component

As an illustration of the influence of the cut-off value on the predicted ductile damage, upsetting of a flange in the setup shown in Fig. 3 is simulated and the results are compared with experimental results in lead by Gouveia et al. [18] showing when and where surface cracks were first observed. After observation of crack initiation, the deformation was stopped. The stress-strain curve of the lead alloy was determined as $\sigma_0 = 66.7 (\bar{\epsilon}^{pl})^{0.10} \text{ MPa}$. The friction factor $m_f = 0.35$ between specimen and tools was determined by ring tests. The flange upsetting was modelled using 6200 quadrilateral elements for fine resolution. The dimensions of the flange and simulation layout can be seen in Fig. 3. Cracks were observed on the outer, peripheral surface of the flange as indicated in Fig. 3c.

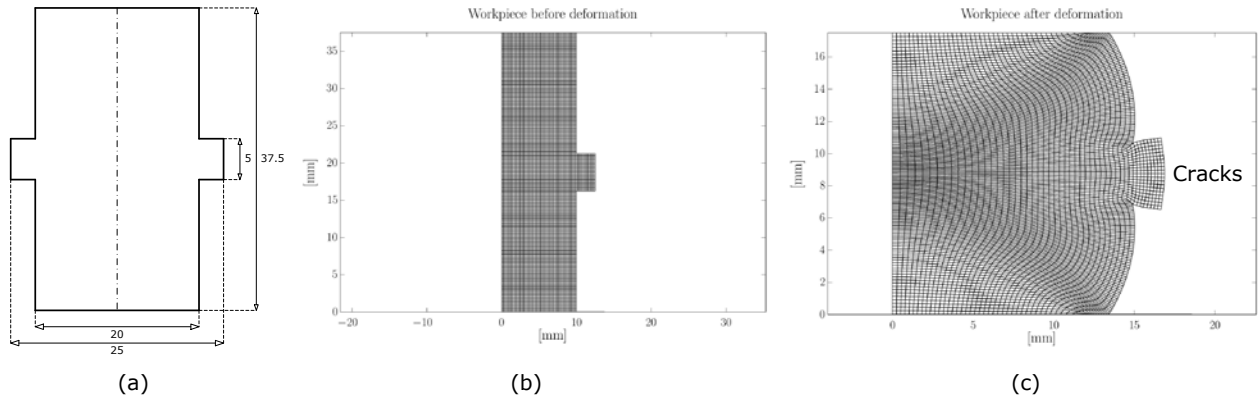


Fig. 3 Flange geometry (a) and mesh before (b) and after compression (c). Almost all numbers and legends on figures are too small, they should be of comparable size as text. This should be revised in all figures

Simulations based on the normalized Cockcroft & Latham and Oyane's criterion for ductile damage are seen in Fig. 4. a_0 is 1 for the Oyane criterion.

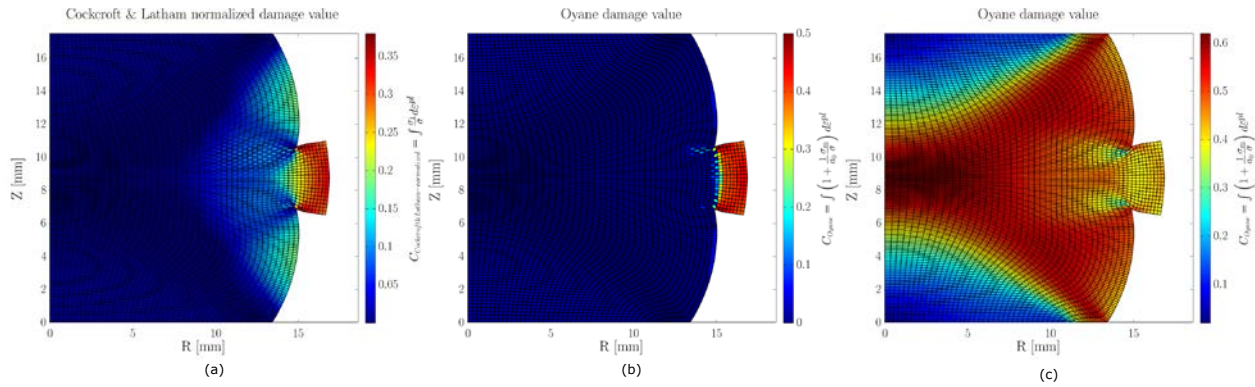


Fig. 4 Predicted Cockcroft & Latham (a) and Oyane damage using cut-off value 1 (b) and 3 (c)

It is seen from Fig. 4 that surface cracks in the flange are predicted by both damage criteria, when applying cut-off value 1. This is in agreement with experimental findings. However when applying cut-off value 3, the Oyane criterion predicts largest damage in the centre of the workpiece and possible cracks on the surface would initiate outside the flange. This is in contradiction to the experimental findings and indicates that care should be taken when implementing ductile damage criteria in numerical software. Gouveia et al. did experiments with several other specimen geometries and compared their results with numerical predictions of surface cracking concluding, that the normalized Cockcroft & Latham and the Oyane criterion, with proper selection of cut-off value, predicted surface crack formation satisfactory.

3.2 Numerical simulation of ingot forging

The numerical simulation is based on a forging process from industry where an ingot 2000mm in diameter is forged between a pair of dies 1000mm wide, giving a width/diameter ratio of 1/2. The simulation is carried out as a 2D plane stress model to reduce computational time. Due to symmetry, only half of the ingot is modelled. 1214 quadrilateral elements are used. The ingot is compressed 200mm (10% of diameter) between two, in the analysis assumed, rigid dies. An example of the simulation layout can be seen in Fig. 5.

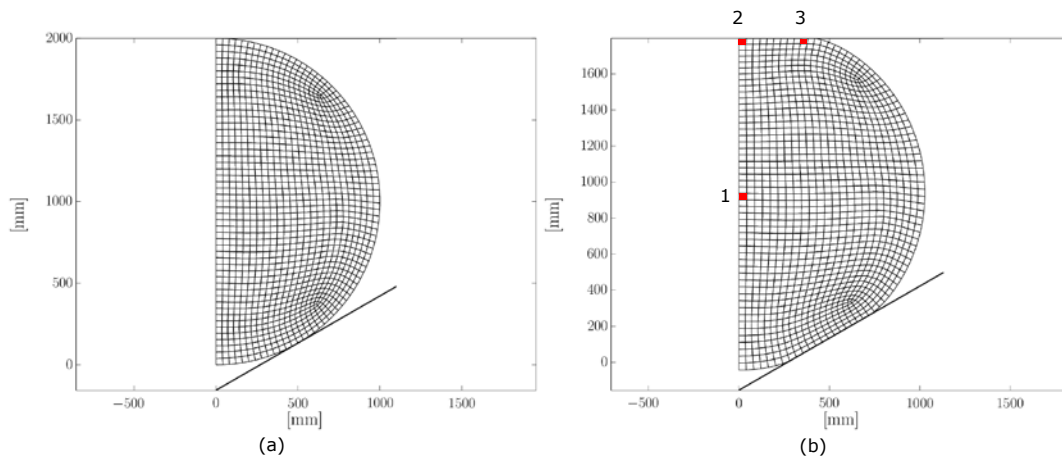


Fig. 5 Ingot before (a) and after compression (b) using a 120° lower die

The purpose of the numerical simulations is to investigate, which of the listed damage criteria is most suited for modelling uncoupled ductile damage in ingot forging and how choice of cut-off value influences the predicted damage. This is done by presenting damage contour plots and by tracking the principal strains of selected elements numbered as 1, 2 and 3 in Fig. 5b.

The ingot material is modelled as rigid-viscoplastic with Norton [19] hardening behaviour:

$$\sigma_0 = C(\dot{\epsilon}^p)^m \quad (8)$$

where σ_0 is the flow stress, C is the strength coefficient and m is the strain-rate exponent. In the simulations C is set to 100MPa, which is a reasonable value for steel at the relevant forging temperature (1200°C) according to Spittel & Spittel [20], and m is either 0.0 or 0.2 to illustrate the influence of strain-rate hardening. Friction is modelled with $m_f = 0.5$. The compression speed of the upper die is 10mm/s, while the lower die remains stationary.

4. Simulation results and discussion

4.1 Stress triaxiality

In order to evaluate the applicability of the different damage criteria, the local stress triaxiality β is calculated in the forged ingot at the end of stroke. Examples of simulations for ideal plastic and strain-rate hardening material can be seen in Fig. 6 and Fig. 7 respectively.

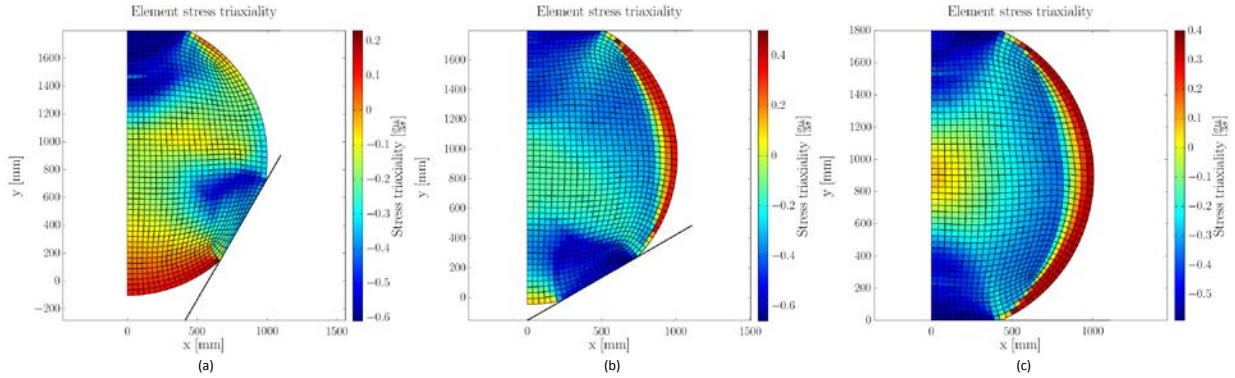


Fig. 6 Stress triaxiality for ingots with flow stress $\sigma_0 = 100 \text{ MPa}$ being forged by 60° (a), 120° (b), and 180° (c) lower die angles

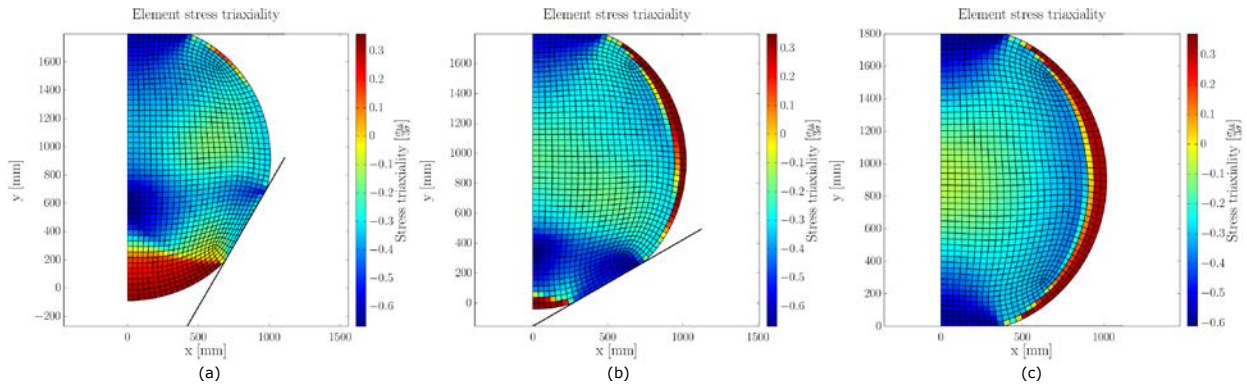


Fig. 7 Stress triaxiality for ingots with flow stress $\sigma_0 = 100 \text{ MPa} \left(\frac{\dot{\epsilon}}{\dot{\epsilon}_{pl}} \right)^{0.2}$ being forged by 60° (a), 120° (b), and 180° (c) lower die angles

It is noticed that a large part of the ingot has negative stress triaxiality in both cases, and to some extent is influenced by strain-rate. This implies that damage criteria like Oyane and Rice & Tracey, depending on choice of cut-off value, may only predict damage in a small part of the ingot. Since the Cockcroft & Latham criterion is able to predict damage even in case of (limited) negative stress triaxiality, it will predict accumulation of damage in larger areas of the ingot. The differences in predicted damage can be seen in a later section.

4.2 Equivalent plastic strain

Since all the listed criteria imply increasing damage with increasing effective plastic strain, this is plotted in Fig. 8 and Fig. 9 for improved understanding of the accumulated damage.

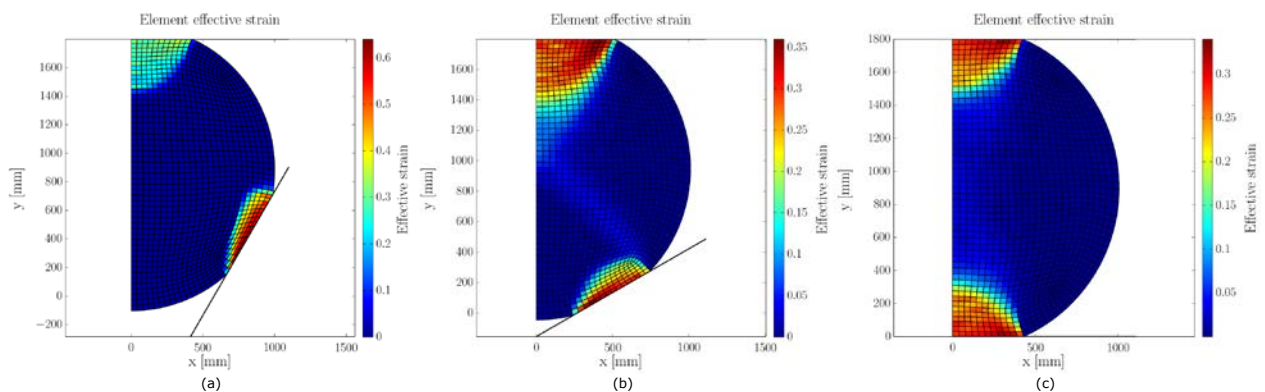


Fig. 8 Effective plastic strain for ingots with flow stress $\sigma_0 = 100 \text{ MPa}$ being forged by 60° (a), 120° (b), and 180° (c) lower die angles

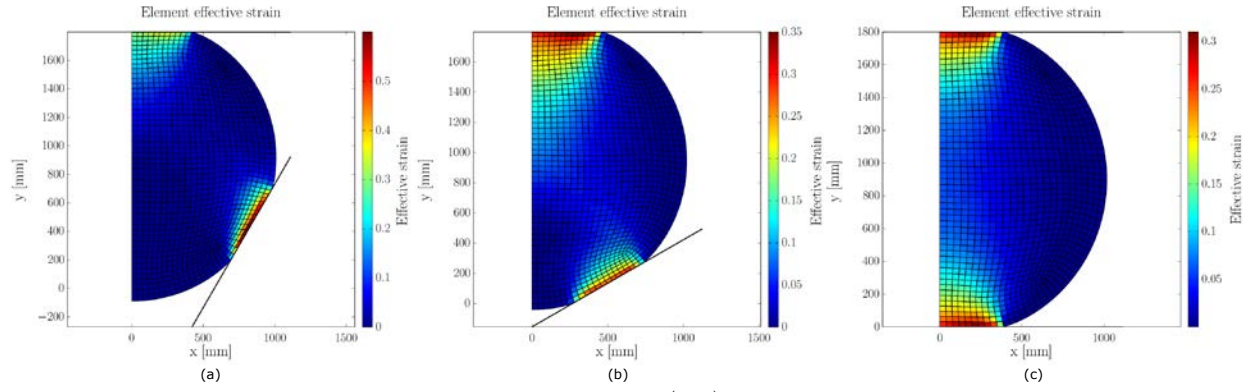


Fig. 9 Effective plastic strain for ingots with flow stress $\sigma_0 = 100MPa(\dot{\epsilon}^{pl})^{0.2}$ being forged by 60° (a), 120° (b), and 180° (c) lower die angles

It is seen that differences in lower die angle result in markedly different plastic strains. The strain-rate sensitive material distributes the accumulated strain (see Fig. 9) more than the constant flow stress material (see Fig. 8) as to be expected.

4.3 Comparison of Cockcroft & Latham and the Oyane ductile damage criterion for cut-off value 1

In this section the predicted ductile damage induced by the forging operation according to the normalized Cockcroft & Latham and the Oyane criterion are compared. The predicted damage by the normalized Cockcroft & Latham criterion can be seen in Fig. 10 and Fig. 11 for ideal plastic and strain-rate sensitive material respectively.

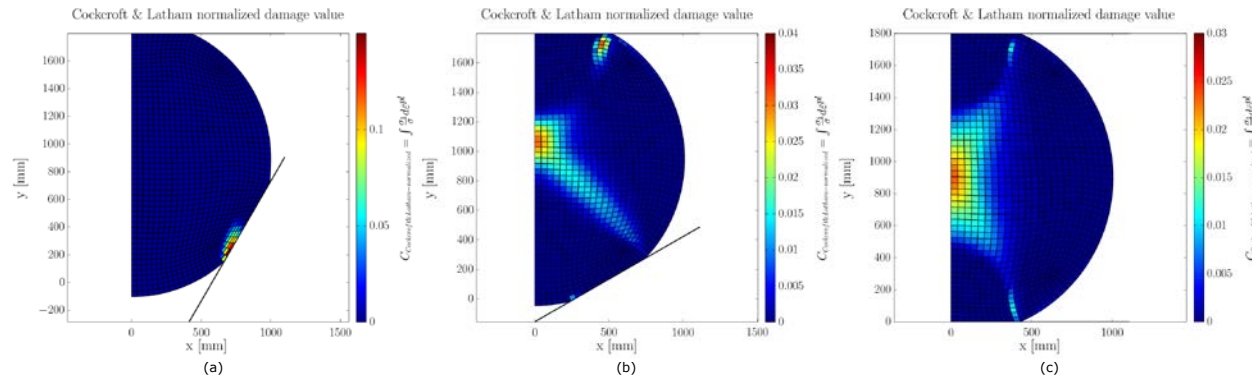


Fig. 10 Cockcroft & Latham criterion for ingots with flow stress $\sigma_0 = 100MPa$ being forged by 60° (a), 120° (b), and 180° (c) lower die angles

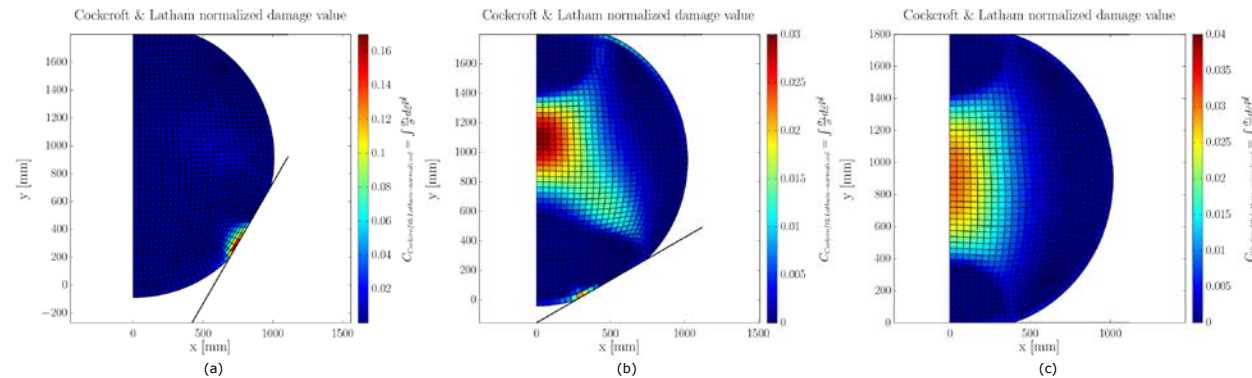


Fig. 11 Cockcroft & Latham criterion for ingots with flow stress $\sigma_0 = 100MPa(\dot{\epsilon}^{pl})^{0.2}$ being forged by 60° (a), 120° (b), and 180° (c) lower die angles

It is seen that the normalized Cockcroft & Latham criteria is quite consistent as regards the predicted location of ductile damage. The strain-rate dependent material distributes the ductile damage more in the cross section of the ingot. This is in accordance with the effective strain distributions shown in Fig. 8 and Fig. 9, which also are more uniformly distributed for the strain-rate hardening material.

The corresponding ductile damage predicted by the Oyane criterion can be seen in Fig. 12 and Fig. 13.

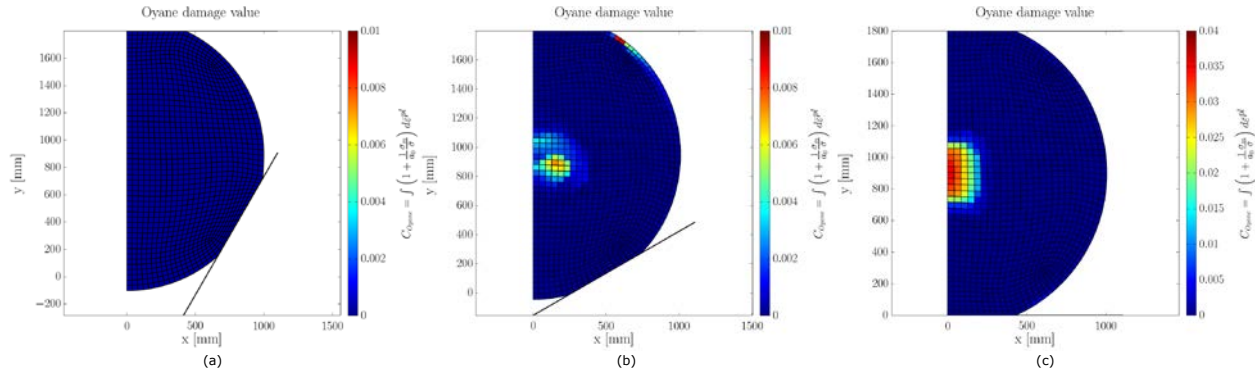


Fig. 12 Oyane criterion for ingots with flow stress $\sigma_0 = 100 \text{ MPa}$ being forged by 60° (a), 120° (b), and 180° (c) lower die angles

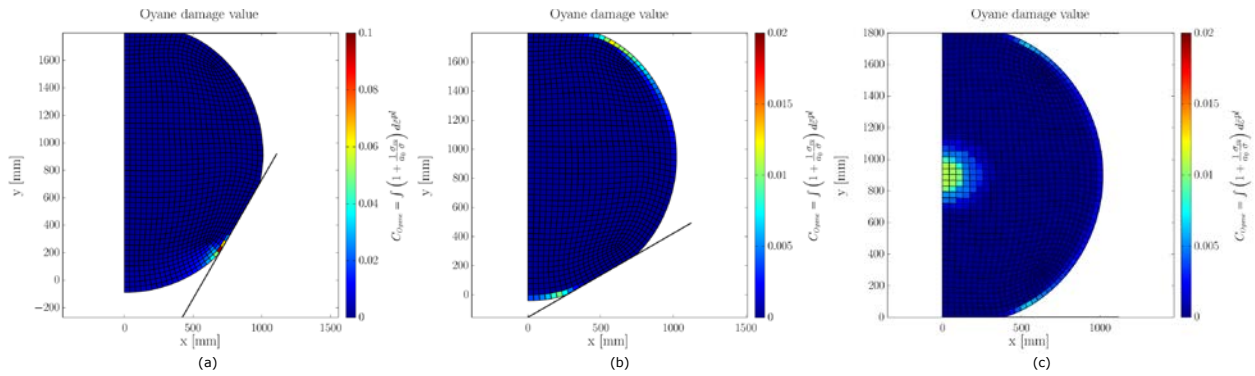


Fig. 13 Oyane criterion for ingots with flow stress $\sigma_0 = 100 \text{ MPa} (\dot{\epsilon}^{pl})^{0.2}$ being forged by 60° (a), 120° (b), and 180° (c) lower die angles

On the contrary to the normalized Cockcroft & Latham criterion, the damage predicted by the Oyane criterion is significantly altered by strain-rate hardening. It does, however, still to some extent agree with the Cockcroft & Latham criterion regarding the location of ductile damage.

4.4 Comparison of Cockcroft & Latham and the Oyane ductile damage criterion for cut-off value 3

If the demand for accumulating damage is changed from cut-off value 1 to 3, the integral in the damage formulation must be positive. This means no significant change in the predicted damage by the Cockcroft & Latham's criterion, but the ones by Oyane and Rice & Tracey are altered. The predicted damage by the Oyane criterion can be seen in Fig. 14 and Fig. 15.

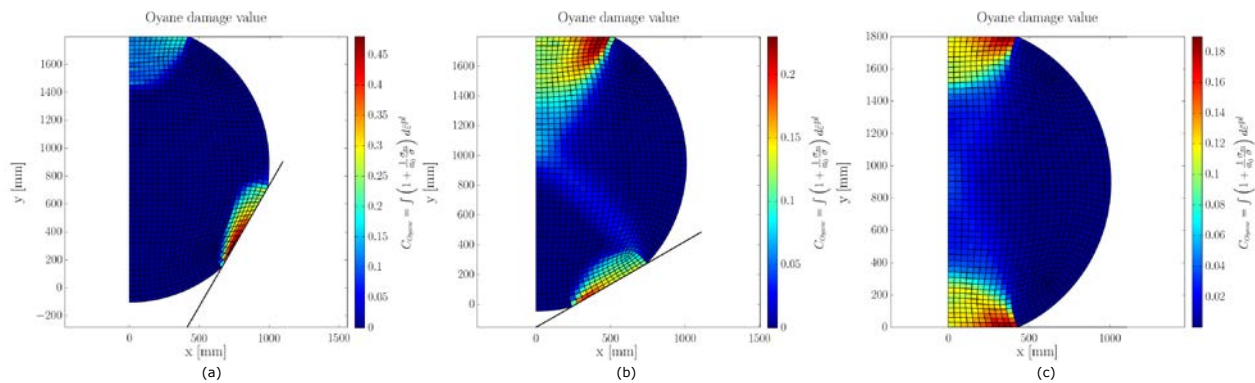


Fig. 14 Oyane criterion for ingots with flow stress $\sigma_0 = 100 \text{ MPa}$ being forged by 60° (a), 120° (b), and 180° (c) lower die angles

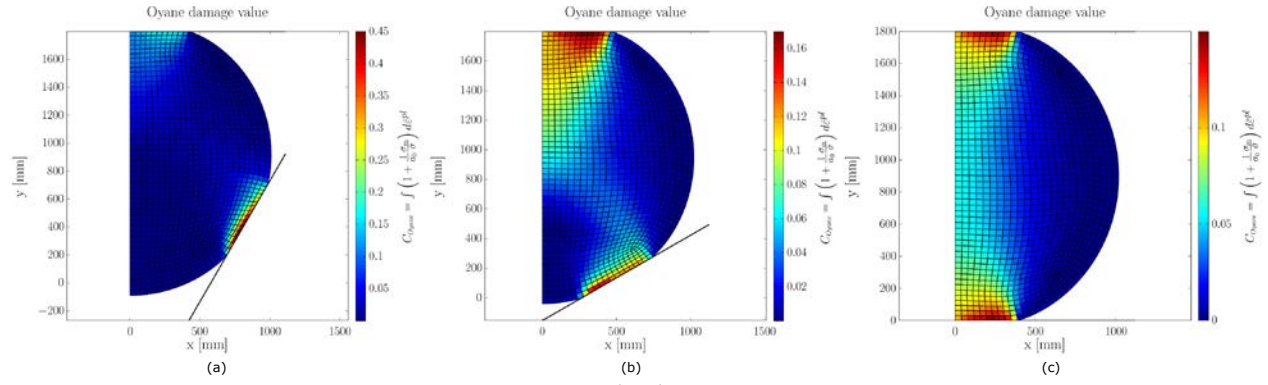


Fig. 15 Oyane criterion for ingots with flow stress $\sigma_0 = 100 \text{ MPa} (\dot{\epsilon}^{pl})^{0.2}$ being forged by 60° (a), 120° (b), and 180° (c) lower die angles

Comparing Fig. 12-13 with Fig. 15 it is noticed that changing the cut-off value for accumulation of damage changes the predicted ductile damage substantially. For a cut-off value of 3 the predicted accumulated damage basically follows the effective plastic strain seen in Fig. 8 and Fig. 9. This is because the stress triaxiality level, seen in Fig. 6 and Fig. 7, is larger than -1, which implies that damage can be accumulated in all elements (when the constant a_0 is set to 1). Since a_0 is determining at lower limit of stress triaxiality at which damage can be accumulated, it is important to obtain this constant experimentally for the ingot material at hand. If a_0 was set to -1/3, the Oyane criterion would predict damage at the same stress triaxiality level as the Cockcroft & Latham criteria for plane stress loading. It is noticed that the predicted damage distribution of the Oyane criterion using cut-off value 3 is quite different from that with cut-off value 1 and also different to the normalized Cockcroft & Latham criterion.

4.5 Element strain loading paths

Principal strains for the three elements shown in Fig. 5 were traced through the deformation process, but only for compression using an 180° lower die. The purpose of this was to identify the deformation history in elements with marked differences in predicted ductile damage location and amount for different choices of cut-off values according to the Oyane criterion. From Fig. 12 and Fig. 13 it is seen that only element number 1 accumulates damage for cut-off value 1. When shifting to cut-off value 3, Fig. 15, more damage is accumulated in element 2 and 3 than in element 1. The recorded strain paths are shown in Fig. 16, where ϵ_{\max} and ϵ_{\min} is the largest and smallest principal strain respectively.

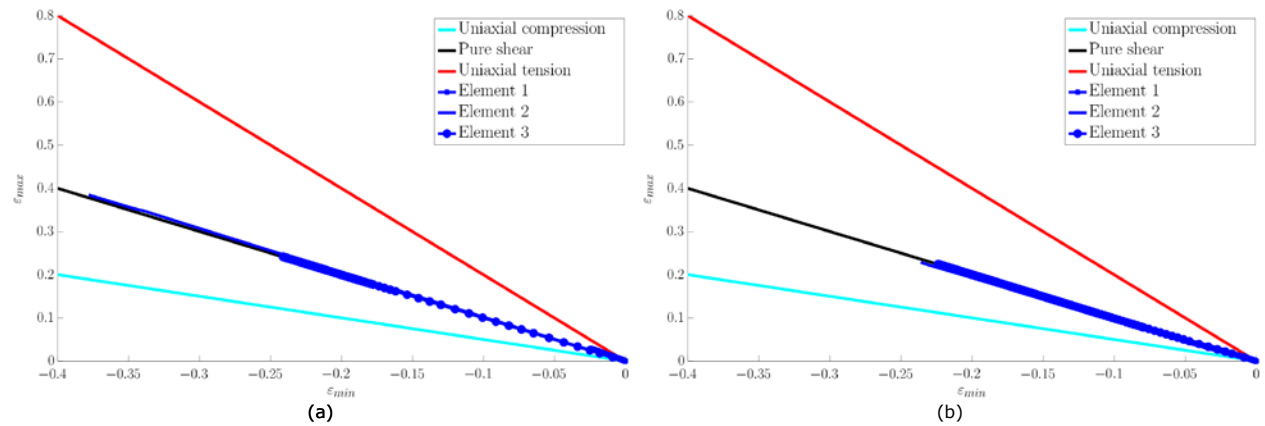


Fig. 16 Strain paths for elements 1-3 when forging ingots with flow stress $\sigma_0 = 100 \text{ MPa}$ (a) and $\sigma_0 = 100 \text{ MPa} (\dot{\epsilon}^{pl})^{0.2}$ (b) with 180° lower die angles

It is noticed that the selected elements 1-3 all have strain paths during loading resembling approximately pure shear deformation. Since pure shear deformation corresponds to $\beta = 0$, it means that the predicted accumulated damage will be sensitive to the choice of cut-off value in these regions in accordance with the discussion in section 2. It is furthermore seen that loading is approximately proportional in the three elements. This justifies the application of Cockcroft & Latham's criterion, since principal stress and strain ratios are constant.

5. Conclusions

A number of different ductile damage criteria have been investigated especially in relation to ingot forging. Among a larger number of damage criteria a few were selected as the most suitable for uncoupled analysis of ductile damage. Their adequacy for modelling a specific, experimental bulk forging formability test was examined.

The combined stress and strain history of ingot forging was analysed. Strain paths of three strategically selected elements were tracked. It was found that the loading in all of these corresponds to almost pure shear deformation. A suitable ductile damage criterion should be able to predict damage for this loading situation. It turned out that the Oyane and the Rice & Tracey criteria were both very sensitive to the programmer's choice of cut-off value for the ingot forging studied, whereas the normalized Cockcroft & Latham criterion was consistent with changing cut-off value. It is furthermore able to predict damage for moderately negative stress triaxialities. If the Oyane criterion is to be applied, careful calibration of the constant a_0 is required.

Acknowledgement

The work is supported by the Strategic Research Center "REWIND - Knowledge based engineering for improved reliability of critical wind turbine components", Danish Research Council for Strategic Research, grant no. 10-093966 Paulo Martins would like to acknowledge the financial support provided by the Velux Foundation during his sabbatical license at the Technical University of Denmark.

References

- [1] J. NASMYTH, "Improvements in forging iron," *Journal of The Franklin Institute*, vol. 50, no. 6, pp. 404-408, 1850.
- [2] H. A. KUHN and C. L. DOWNEY, "Deformation characteristics and plasticity theory of sintered powder materials," *Int. J. Powder Met.*, vol. 7, no. 1, pp. 15-25, 1971.
- [3] R. GREEN, "A plasticity theory for porous solids," *Int. J. of Mech. Sci.*, vol. 14, no. 4, pp. 215-224, 1972.
- [4] V. TVERGAARD and A. NEEDLEMAN, "Analysis of the cup-cone fracture in a round tensile bar," *Acta Metallurgica*, vol. 32, pp. 157-169, 1984.
- [5] L. KACHANOV, "Time of the rupture process under creep conditions," *Izv. Akad. Nauk. SSR. Otd. Tekh. Nauk*, vol. 8, pp. 26-31, 1958.
- [6] LEMAITRE, "A continuous damage mechanics model for ductile fracture," *Trans. ASME, J. Eng. Mater. Technol.*, vol. 107, no. 1, pp. 83-89, 1985.
- [7] L. XUE and T. WIERZBICKI, "Ductile fracture initiation and propagation modeling using damage plasticity theory," *Engineering Fracture Mechanics*, vol. 75, no. 11, pp. 3276-3293, 2006.
- [8] A. M. FREUDENTHAL, *The inelastic behavior of engineering materials and structures*, 1. ed., John Wiley & Sons Ltd., 1950.
- [9] M. C. COCKCROFT and D. J. LATHAM, "Ductility and workability of metals," *Journal of the Institute of Metals*, vol. 96, pp. 33-39, 1968.
- [10] M. OYANE, "Criteria of ductile fracture strain," *Bull. Jpn. Soc. Mech. Eng. (Japan) Bulletin of JSME*, vol. 15, no. 90, pp. 1507-1513, 1972.
- [11] J. R. RICE and D. M. TRACEY, "On the ductile enlargement of voids in triaxial stress fields," *Journal of the Mechanics and Physics of Solids*, vol. 17, pp. 201-17, 1969.
- [12] P. BROZZO, B. DELUCA and R. RENDINA, "A new method for the prediction of formability limits of metal sheets," *Sheet Metal Forming and Formability - Proceedings of the Seventh Biennial Congress of International Deep Drawing Research Group*, 1972.
- [13] M. AYADA, T. HIGASHINO and K. MORI, "Central bursting in extrusion of inhomogeneous materials," *Proceedings of the First ICTP. Adv. Technol. of Plast.*, vol. 1, pp. 553-558, 1984.
- [14] P. W. BRIDGMAN, "Effects of high hydrostatic pressure on the plastic properties of metals," *Rev. Mod. Phys. (USA)*, vol. 17, pp. 3-14, 1945.
- [15] DEFORM, DEFORM v10.2.1 - INTEGRATED 2D3D SYSTEM MANUAL, Ohio: DEFORM, 2012.
- [16] VUJOVIC and SHABAIK, "A new workability criterion for ductile metals," *Trans. ASME, J. Eng. Mater. Technol.*, vol. 108, no. 3, pp. 245-249, 1986.
- [17] C. V. NIELSEN, W. ZHANG, L. M. ALVES, N. BAY and P. A. F. MARTINS, *Modeling of Thermo-Electro-Mechanical Manufacturing Processes*, 1. ed., Springer, 2013.
- [18] B. P. P. A. GOUVEIA, J. M. C. RODRIGUES and P. A. F. MARTINS, "Fracture prediction in bulk metal forming," *Int. J. Mech. Sci.*, vol. 38, pp. 361-372, 1996.
- [19] F. H. NORTON, *The Creep of Steel at High Temperatures*, 1. ed., McGraw-Hill, 1929.
- [20] M. SPITTEL and T. SPITTEL, "Steel symbol/number: 42CrMo4/1.7225," in *Landolt-Börnstein - Group VIII Advanced Materials and Technologies*, vol. 2C1, Springer-Verlag Berlin Heidelberg, 2009.
- [21] S. SEMIATIN, Ed., *ASM Handbook - Volume 14A, Metalworking: Bulk Forming*, ASM, 2005.

